Common Volatility in Emerging Markets: Sources and Spillovers

Amanda Seixas Diniz[a]
João Victor Issler[†, a]

[a]EPGE FGV

Abstract This paper investigates the determinants of common volatility (COVOL) in emerging markets. Unlike the existing literature, we incorporate the stochastic discount factor of Araujo, Galvão, and Issler (2024) as the common factor in the conditional mean of returns. We find that episodes of elevated emerging market COVOL are predominantly associated with oil market shocks — differing from Engle and Campos-Martins (2023), whose global sample assigns a less central role to this factor — with oil-producing and oil-exporting countries exhibiting the greatest sensitivity. Examining the relationship between emerging market COVOL, its developed market counterpart, Brent returns, and the VIX via TVP-VAR, we find that emerging market COVOL acts, on net, as a receiver of shocks, and that total connectedness intensifies during periods of global stress. These findings suggest that emerging market common volatility is driven by a distinct set of forces and remains systematically subordinate to developed market risk, with integration that tightens precisely when diversification benefits would be most valuable.

Keywords: COVOL; Emerging markets; TVP-VAR; Connectedness; Risk Transmission.

JEL codes: G15, F36, C32, C48.

1. Introduction

What events drive common volatility in emerging markets? Among both market practitioners and academic researchers, there is broad consensus that assets traded in emerging economies exhibit dynamics that differ markedly from those of their developed market counterparts. As documented by Bekaert and Harvey (1997), the main distinguishing features are higher average returns, low correlations with developed market returns, and greater volatility. These characteristics generally reflect a combination of weak macroeconomic fundamentals, dependence on external capital flows, underdeveloped financial markets, and

amanda.diniz@fgv.br
[†]joao.issler@fgv.br

elevated institutional and political risk.

Regarding volatility in particular, Aggarwal, Inclan, and Leal (1999) show that it displays distinct properties in emerging markets, including greater persistence and heightened sensitivity to local shocks relative to global factors. Moreover, even as financial integration has deepened, Bekaert and Harvey (2023) reaffirm that emerging markets continue to differ substantially from developed ones, notwithstanding the advances in financial globalization. The authors note that, while these markets have become more correlated with developed markets over time, they retain distinct risk-return profiles — particularly under alternative portfolio constructions that depart from market-capitalization-weighted benchmarks.

Although these characteristics are well established in the literature, most studies examine the volatility of individual emerging economies in relative isolation, without investigating whether a common force drives them simultaneously. This approach, however, leaves open a relevant question: if these markets share similarly fragile fundamentals and structural vulnerabilities, to what extent is their volatility affected jointly? That is, beyond country-specific idiosyncratic volatility, is there a common factor that induces comovement in the volatility of emerging market assets? Identifying and characterizing this common factor is the central objective of this paper.

Engle and Campos-Martins (2023) proposed a risk measure termed COVOL, which captures the common volatility across a given set of assets and each asset's sensitivity to that common component. This measure provides a tractable framework for quantifying risk sharing and volatility comovement, and is directly applicable to the emerging market context. In their original study, the authors estimated COVOL across 47 countries — 23 developed and 24 emerging — yielding a global measure of common volatility. Their results indicate that, over the past two decades, the episodes that most intensified this global volatility were those associated with the COVID-19 pandemic and events of a political and military nature.

This raises a natural question: whether the common volatility of emerging markets follows the same dynamics as its global counterpart, or whether it exhibits a structure of its own, not fully accounted for by the factors governing developed markets. To investigate this ques-

tion, we estimate separate COVOLs for the two groups of markets and examine the extent to which emerging market COVOL is driven by developed-market factors, by surges in uncertainty, and by oil market shocks — whose relevance becomes apparent from inspection of the extreme values of the series. Specifically, and in line with the findings of Bekaert and Harvey (2023), we are interested in whether this relationship is stable over time or whether risk transmission between the two groups has intensified — or attenuated — in response to specific episodes of global stress.

To address this question, we employ a time-varying parameter vector autoregression (TVP-VAR) with connectedness indices computed via generalized forecast error variance decomposition, following Diebold and Yılmaz (2014) as implemented in Koop and Korobilis (2013). The system includes, alongside the two COVOL series, Brent oil returns and the VIX. This specification allows us to identify the extent to which emerging market common volatility is driven by each factor and how the connectedness among them has evolved over time.

The results indicate that emerging market COVOL acts predominantly as a net receiver of shocks within the system, with developed market COVOL accounting for the largest share of its forecast error variance among the external variables. Total system connectedness, as measured by the TCI, is not constant over time: it rises sharply during episodes of global stress — most notably the 2008 financial crisis and the COVID-19 pandemic — and recedes during periods of greater stability. This pattern suggests that emerging market exposure to global risk expands precisely at the moments when international diversification would be most valuable.

This paper also estimates COVOL using the stochastic discount factor of Araujo, Galvão, and Issler (2024) as the common factor in the conditional mean equation for returns. Existing specifications tie factor identification to choices about the underlying pricing model — such as the first principal component in Engle and Campos-Martins (2023) or the Fama-French factors in Campos-Martins and Hendry (2024) — whereas the estimator of Araujo, Galvão, and Issler (2024) is constructed exclusively from cross-sectional returns, without imposing assumptions about preferences or risk aversion parameters. This choice anchors the specification in no-arbitrage foundations and yields a more

parsimonious identification of the emerging market COVOL.

The remainder of the paper is organized as follows. Section 2 reviews the related literature and details the specific contributions to each strand. Section 3 describes the methodological framework, covering the estimation of COVOL and the TVP-VAR model. Section 4 reports the empirical results, including the analysis of the properties of emerging market COVOL, the dynamic connectedness indices, and their variation over the global financial cycle. Section 5 concludes.

2. Related Literature

This paper contributes to three strands of the literature. The first concerns the measurement and characterization of common volatility in financial markets, building on Engle and Campos-Martins (2023). Subsequent studies have extended this framework to specific contexts: Campos-Martins and Hendry (2024) applied the model to the oil and gas sector to measure industry-wide common movements and identify those driven by unexpected increases in climate change concerns, while Chen et al. (2025) estimated common volatility in energy commodity markets and its effects on sectoral connectedness in the Chinese equity market. In parallel, Lang et al. (2024a) and Ben Jabeur, Bakkar, and Cepni (2025) explored COVOL as an explanatory variable in risk transmission to financial markets and clean energy markets, respectively. The present paper advances this agenda by estimating COVOL separately for emerging and developed markets, documenting the properties of emerging market common volatility as a group-specific factor — an extension that, to the best of our knowledge, has not been undertaken in the literature.

The second strand is the literature on risk transmission, which can be divided into two fronts that converge on the object of this paper. The first covers the design of dynamic connectedness measures. Gabauer and Gupta (2018) introduced a group-specific decomposition of the Diebold-Yilmaz indices within the TVP-VAR framework, allowing domestic spillovers to be separated from international ones and documenting asymmetric transmission of economic uncertainty between the United States and Japan. Feng, Shi, and Kutan (2025) extend the

analysis of regional equity market volatility forecasting beyond the VIX, documenting asymmetric fear spillovers across implied volatility indices and showing that the COVID-19 pandemic shifted predictive power from the VIX toward the Chinese volatility index.

The second front incorporates the COVOL of Engle and Campos-Martins (2023) as a measure of global systemic risk. Xu, Hu, Corbet, et al. (2023) investigate the dynamic connectedness between global COVOL and four implied volatility indices, documenting that COVOL acts predominantly as a receiver of volatility transmissions. Lang et al. (2024b) show that COVOL receives transmissions from North American and European equity markets, and that connectedness intensifies during stress episodes such as the global financial crisis and the pandemic. Xu, Hu, Oxley, et al. (2025) broaden the scope by incorporating ESG markets from both developed and emerging economies, finding that the developed group dominates the transmission channel and that COVOL behaves as a net receiver within the aggregate ESG system. Also at the emerging-developed frontier, Babar, Ahmad, and Yousaf (2024) document weak connectedness between agricultural commodities and emerging equity indices, with the latter positioned predominantly as net receivers of volatility.

Despite this progress, the literature has yet to examine the dynamic relationship between common volatility factors estimated separately for the universe of developed and emerging markets. This paper fills that gap by directly modeling the time-varying transmission between emerging market COVOL and developed market COVOL via TVP-VAR with Diebold-Yilmaz indices based on GFEVD, documenting how the direction and intensity of connectedness between these factors vary over the global financial cycle — including the 2008 financial crisis, the 2014–2016 commodity market downturn, and the COVID-19 pandemic.

Finally, the third strand concerns the specification of the common factor used in the conditional mean equation for returns, a prior and necessary step for COVOL estimation. Engle and Campos-Martins (2023) employ the first principal component of the return matrix and the return on a global market index, while Campos-Martins and Hendry (2024) adopt the Fama-French factors augmented with WTI oil returns — specifications that tie factor identification to choices about the under-

lying pricing model. This paper adopts the estimator of Araujo, Galvão, and Issler (2024) for the stochastic discount factor, constructed from cross-sectional returns without requiring assumptions about preferences or risk aversion parameters. This specification anchors the factor in no-arbitrage foundations without imposing additional parametric structure, yielding a more parsimonious identification of emerging market COVOL.

3. Methodology

Volatility in emerging markets is shaped by a complex interplay of domestic vulnerabilities and external shocks. To investigate these dynamics, we implement a two-step methodology. In the first step, we estimate common volatility (COVOL) series for each market group separately, following the multiplicative factor decomposition framework of Engle and Campos-Martins (2023). In the second step, these series are incorporated into a TVP-VAR, from which we construct dynamic connectedness measures between the two blocs over time. The remainder of this section describes each step in turn.

3.1 Asset returns and factor models

Estimating the common volatility factor requires that the conditional mean of each return series be filtered out via a factor model, and that the resulting residuals be standardized by their individual conditional variances. To set up the model, consider $\mathbf{r}_t = (r_{1,t}, r_{2,t}, \ldots, r_{N,t})'$ denote the $(N \times 1)$ vector of returns for country-specific ETFs, where each return is defined as $r_{i,t} = (p_{i,t} + d_{i,t})/p_{i,t-1}$, with $p_{i,t}$ and $d_{i,t}$ representing, respectively, the closing price and dividend paid in period t. Following the standard formulation of multivariate volatility models as in Engle and Campos-Martins (2023), we assume the following conditional moments:

$$\mathbb{E}_{t-1}(\mathbf{r}_t) = \boldsymbol{\mu}_t, \tag{1}$$

$$\mathbb{E}_{t-1}[(\mathbf{r}_t - \boldsymbol{\mu}_t)(\mathbf{r}_t - \boldsymbol{\mu}_t)'] = H_t. \tag{2}$$

Accordingly, we define the jointly standardized residuals as $\mathbf{e}_t = H_t^{-1/2}(\mathbf{r}_t - \boldsymbol{\mu}_t)$. If the model is correctly specified, it follows that:

$$\mathbb{E}_{t-1}(\mathbf{e}_t \mathbf{e}_t') = \mathbb{I}, \tag{3}$$

$$\mathbb{E}_{t-1}[(\mathbf{e}_t^2 - \boldsymbol{\iota})(\mathbf{e}_t^2 - \boldsymbol{\iota})'] = \boldsymbol{\Psi}_t, \tag{4}$$

where $\boldsymbol{\iota}$ is a vector of ones. This structure is particularly useful because, analogously to univariate (G)ARCH models, it allows a multiplicative decomposition of the volatility factor. Moreover, the framework permits second-moment comovements (i.e., contemporaneous correlation of volatility shocks) across assets without compromising the consistency of parameter estimates.

Following Engle and Campos-Martins (2023), we now build on this framework by specifying the asset pricing model as:

$$\mathbf{f}_t = \mathbf{w}_{t-1}' \mathbf{r}_t, \tag{5}$$

$$\mathbf{r}_t = r^f + \boldsymbol{\beta} \mathbf{f}_t + \operatorname{diag}\left(\sqrt{\mathbf{h}_t^i}\right) \mathbf{e}_t^i, \tag{6}$$

where $\mathbf{f}_t$ is the $(K \times 1)$ vector of factors, constructed as a linear combination of the asset returns with weights $\mathbf{w}_{t-1}$; r^f is the risk-free rate; $\boldsymbol{\beta}$ is the $(K \times K)$ matrix of factor loadings; and $\mathbf{h}_t^i$ denotes the conditional variance associated with asset i. This formulation preserves the multiplicative volatility structure that characterizes GARCH models, while allowing for heterogeneity and comovement in the idiosyncratic shocks. Hence, under correct model specification, the idiosyncratic residuals are uncorrelated both over time and across assets, with unit variances.

The factors $\mathbf{f}_t$, in turn, are constructed as linear combinations of returns and therefore exhibit conditional volatilities and residuals. Assuming that these factors can be rotated to form an orthogonal basis, the conditional covariance matrix H_t^f becomes diagonal, implying that factor residuals are uncorrelated both among themselves and with the idiosyncratic residuals e_t^i. Furthermore, we assume that the selected factors are sufficient to capture the common risk structure; otherwise,

the idiosyncratic components may exhibit cross-sectional correlation, violating the fundamental assumptions of the covolatility model.

Thus, the specification of the functional form for both the conditional mean and variance plays a crucial role in accurately measuring volatility comovements across countries. Following the framework proposed by Engle and Campos-Martins (2023) and Campos-Martins and Hendry (2024), the model is given by:

$$r_{i,t} = r^f + \delta_i r_{i,t-1} + \boldsymbol{\beta}_i' \mathbf{f}_t + u_{i,t} \tag{7}$$

$$u_{i,t} = h_{i,t} e_{i,t} \tag{8}$$

$$h_{i,t} = \omega_i + \alpha_{i,h} u_{i,t}^2 + \beta_{i,h} h_{i,t-1}. \tag{9}$$

To ensure positivity of the conditional variance and the stationarity of the GARCH process, the following parameter restrictions are imposed: $\omega_i, \alpha_{i,h} > 0$, $\beta_{i,h} \geqslant 0$, and $\alpha_{i,h} + \beta_{i,h} < 1$. The model combines an AR(1) structure for the conditional mean of returns with a GARCH(1,1) process for the conditional variance of the idiosyncratic shocks. Regarding the common factors, Engle and Campos-Martins (2023) consider two: (i) the first principal component extracted from the asset return matrix, and (ii) the return of a global market index. Campos-Martins and Hendry (2024), in turn, use: (i) the three classical Fama-French factors, and (ii) the excess return of WTI crude oil.

This formulation is based on the CAPM framework, which assumes that systematic risk is fully captured by market fluctuations within a general equilibrium setting for asset pricing. However, alternative models such as the Fama-French three- and five-factor models propose that accounting variables and market capitalization characteristics also reflect relevant sources of systematic risk.

Given the diversity of specifications proposed in the literature, we have the parsimonious proposal by Araujo, Galvão, and Issler (2024) – AGI. The authors develop a consistent estimator for the stochastic discount factor (SDF), denoted by M_t, using only asset return data, with no need for utility function assumptions or risk-aversion parameters. Their approach relies on a no-arbitrage, log-linear one-factor model where the log of the SDF itself serves as the common factor:

$$r_{i,t} = r_t^f + \beta_{i,AGI}\hat{M}_t + u_{i,t} \tag{10}$$

$$\hat{M}_t = \frac{\overline{R}_t^G}{\frac{1}{T}\sum_{j=1}^{T} \overline{R}_j^G \overline{R}_j^A} \tag{11}$$

where $\overline{R}_t^A$ denotes the arithmetic mean of cross-sectional returns in period t, whereas $\overline{R}_j^G$ represents the geometric mean of their reciprocals, with equal weighting across assets.

While cross-sectional return variation provides a biased estimate of the SDF, this bias is corrected using time-series variation. Issler, Martins, and Moog (2024) showed that the one-factor model outperforms the CAPM, Fama-French three- and five-factor models, and Lettau and Ludvigson's cay specifications — in explaining the cross-section of returns through Fama-MacBeth regressions. The model achieved the best fit for the 25 Fama-French portfolios using both monthly and quarterly data.

In order to assess the sensitivity of results to the choice of factor, we estimate the COVOL model under both the AGI specification and the original specification of Engle and Campos-Martins (2023) over the same sample, which allows a direct comparison of each approach's ability to capture the covolatility structure of emerging and developed markets. Figure 1 displays the COVOL estimates under both specifications across the full sample period.

Figure 1
Emerging market COVOL estimates under different specifications

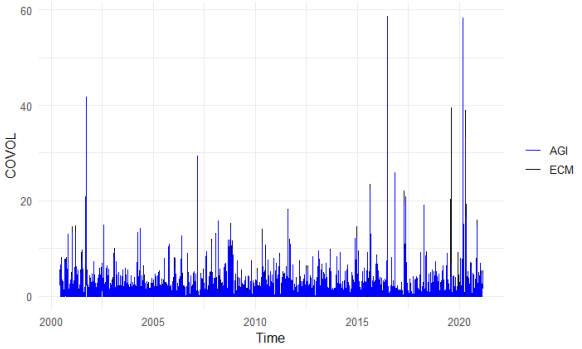

The series exhibit similarity in both magnitude and timing, with a correlation coefficient of 0.9552, indicating the consistency of common volatility identification across methodological approaches. Table A2 corroborates this finding by presenting the twenty most extreme volatility realizations identified by each specification, revealing considerable overlap in the timing and ranking of major market stress episodes. Among the twenty extreme events identified, only three differ between specifications (highlighted in red - table A2), while two additional episodes differ by merely one day (highlighted in blue).

The factor loading estimates presented in Table A1 also demonstrate a clear similarity between the ECM and AGI specifications in terms of country rankings and relative magnitudes. Both approaches identify European markets as the most exposed to the common volatility factor, with France, Spain, Italy, and Germany consistently occupying the top positions across specifications. The similarity between specifications also holds in the identification of countries with lower exposure to the common volatility factor. Economies such as India, Turkey, Vietnam, Poland, and New Zealand are placed at the bottom of the distribution under both models, with loadings below 0.10.

Therefore, we adopt the AGI specification, as these results provide robust empirical support for its use as the common factor in the COVOL framework. Moreover, its identification rests exclusively on the asset pricing equation and the cross-sectional mean structure of

returns — without relying on consumption data, functional form assumptions on preferences, or risk aversion parameters —, which rules out misspecification arising from the choice of preference model and avoids the puzzles documented in the consumption-based asset pricing literature.

3.2 Modeling common volatility

After modeling and filtering the common risk structure across emerging markets, the next step is to characterize their common variance factor. Following the notation in Engle and Campos-Martins (2023), we define the COVOL as a latent variable, denoted as $\sqrt{x_t}$, where $x = (x_1, \ldots, x_T)'$ is a $T \times 1$ vector. Let $s = (s_1, \ldots, s_N)'$ denote the $N \times 1$ vector of factor loadings, which capture the sensitivity of each country to aggregate volatility shocks.

We formalize the stochastic properties of x_t and the idiosyncratic disturbances as follows:

$$\begin{aligned} \mathbb{E}_{t-1}(x_t) &= 1, \\ \mathbb{E}_{t-1}(x_t - 1)^2 &= v_t, \quad x_t > 0, \quad t = 1, \ldots, T, \\ \varepsilon_{i,t} &\sim IIN(0,1), \\ s_i &\in [0,1], \quad i = 1, \ldots, N. \end{aligned}$$

We further assume that x_t is strictly positive and independent from the idiosyncratic errors $\varepsilon_{i,t}$. Under these conditions, the standardized residuals for country i at time t take the form:

$$e_{i,t} = \sqrt{g(s_i, x_t)}\varepsilon_{i,t}, \tag{12}$$

where $g(s_i, x_t)$ is the data-generating process for $e_{i,t}$ from x_t and s_i. The parameter s_i can be interpreted as a country-specific fixed effect that governs exposure to the common volatility factor.

Following the authors, we adopt the functional form $g(s_i, x_t) \equiv s_i(x_t - 1) + 1$, which ensures $g(s_i, x_t) \geqslant 0$ for all t and $\mathbb{E}[g(s_i, x_t)] = 1$.

This normalization guarantees that $\mathbb{E}_{t-1}(\mathbf{e}_t \mathbf{e}_t') = \mathbb{I}$, thus preserving a standardized covariance structure.

The authors demonstrate that, assuming x_t has strictly positive variance, the covariance matrix of the squared residuals, $\mathbf{e}_t^2$, becomes non-diagonal. This reflects positive correlations between $e_{i,t}^2$ and $e_{j,t}^2$ for different assets $i \neq j$ within the same period t. The theoretical relationship is given by:

$$\begin{aligned} \mathbb{E}_{t-1}\left[(e_{i,t}^2 - 1)(e_{j,t}^2 - 1)\right] &\equiv \Psi_{ij,t} = s_i s_j v_t, \\ \mathbb{E}_{t-1}\left[(e_{i,t}^2 - 1)^2\right] &\equiv \Psi_{ii,t} = 3s_i^2 v_t + 2. \end{aligned} \tag{13}$$

Based on these expressions, the conditional covariance matrix Ψ can be constructed as:

$$\begin{aligned} \Psi &= \frac{1}{T}\mathbb{E}\left[\sum_{t=1}^{T} \mathbf{e}_t^2 \mathbf{e}_t^{2\prime}\right] = \frac{1}{T}\sum_{t=1}^{T} \Psi_t = \mathbf{s}\mathbf{s}'\bar{v} + D, \\ D &= \operatorname{diag}\left\{3s_i^2 \bar{v} + 2\right\}, \end{aligned} \tag{14}$$

where $\bar{v} = \frac{1}{T}\sum_{t=1}^{T} v_t$. The presence of co-movements (COVOL) is tested by examining the diagonal structure of the covariance matrix Ψ. Under the alternative hypothesis, time variation in x_t induces positive correlation in $\mathbf{e}_t^2$, leading to a non-diagonal covariance matrix.

To test for the existence of COVOL, Engle and Campos-Martins (2023) assume that all s_i, for $i = 1, \ldots, N$, are equal under the alternative hypothesis. This implies that all assets are equally affected by a common volatility shock. Imposing this restriction enables an asymptotically optimal test, yielding greater statistical power than would be achieved under heterogeneous factor loadings. Therefore, the null hypothesis tests for the absence of equicorrelation in the panel:

$$\mathbb{H}_0 : \rho_{\mathbf{e}^2} = 0 \quad \text{versus} \quad \mathbb{H}_1 : \rho_{\mathbf{e}^2} > 0.$$

The proposed test statistic is:

$$\xi = \frac{\sqrt{\frac{NT}{(N-1)/2}} \sum_{i>j,j=1}^{N} \sum_{t=1}^{T} (e_{i,t}^2 - 1)(e_{j,t}^2 - 1)}{\sum_{i=1}^{N} \sum_{t=1}^{T} (e_{i,t}^2 - 1)^2}, \tag{15}$$

which converges to a standard normal distribution under $\mathbb{H}_0$.

The next step involves estimating the model, that is, obtaining the estimates for x_t and $\mathbf{s}$. Engle and Campos-Martins (2023), under the assumption of normality, propose the following log-likelihood function:

$$L(s,x;e) = -\frac{1}{2} \sum_{i=1}^{N} \sum_{t=1}^{T} \left\{ \log[g(s_i,x_t)] + \frac{e_{it}^2}{g(s_i,x_t)} \right\}. \tag{16}$$

This does not correspond to a standard likelihood function, as both the parameter vector $\mathbf{s}$ and the latent variable x_t are unknown. Consequently, estimation proceeds by maximizing this function through an alternating procedure: estimating $\mathbf{s}$ conditional on $\hat{x}$ using time-series analysis, and estimating x conditional on $\hat{\mathbf{s}}$ using cross-sectional analysis. The associated first-order conditions are:

$$\begin{aligned} \frac{\partial L(s,x;e)}{\partial s_i} &= 0 \\ \frac{\partial L(s,x;e)}{\partial x_t} &= 0. \end{aligned} \tag{17}$$

The estimation begins with an initial value of the matrix $\mathbf{\Psi}$ obtained through principal component analysis. An iterative process is then implemented, alternating between the cross-sectional and time-series estimations until the log-likelihood function $L(s,x;e)$ converges to its maximum. This estimation routine is performed using the Expectation-Maximization (EM) algorithm.

3.3 Dynamic connectedness via TVP-VAR

The connectedness analysis draws on the TVP-VAR framework of Antonakakis, Chatziantoniou, and Gabauer (2020), which combines

the variance decomposition approach of Diebold and Yılmaz (2014) with a time-varying covariance structure estimated via Kalman filter. Relative to the conventional rolling-window VAR, this specification tracks structural shifts in the data more precisely and retains the full sample throughout estimation. The TVP-VAR(p) model takes the form

$$y_t = A_t z_{t-1} + e_t, \qquad e_t \mid \Omega_{t-1} \sim \mathcal{N}(0, \Sigma_t), \tag{18}$$

$$\text{vec}(A_t) = \text{vec}(A_{t-1}) + \xi_t, \qquad \xi_t \mid \Omega_{t-1} \sim \mathcal{N}(0, \Xi_t), \tag{19}$$

where Ω_{t-1} is the information set at $t-1$; y_t and z_{t-1} are $m \times 1$ and $mp \times 1$ vectors; A_t is an $m \times mp$ coefficient matrix; and Σ_t, Ξ_t are time-varying variance-covariance matrices of dimensions $m \times m$ and $m^2 p \times m^2 p$, respectively.

The filter is initialized with OLS estimates from the first T_0 observations, following Primiceri (2005) and Del Negro and Primiceri (2015): $\text{vec}(A_0) \sim \mathcal{N}(\text{vec}(\hat{A}^{\text{OLS}}), \hat{\Sigma}^A_{\text{OLS}})$ and $\Sigma_0 = \hat{\Sigma}_{\text{OLS}}$. Estimation employs forgetting factors $\kappa_1 = 0.99$ and $\kappa_2 = 0.96$, set at the values recommended by Koop and Korobilis (2014); Koop and Korobilis (2013) document that time-varying decay factors do not improve forecast accuracy and impose a substantial computational cost.

In the prediction step of the multivariate Kalman filter, the relevant quantities are:

$$A_{t|t-1} = A_{t-1|t-1}, \tag{20}$$

$$\Sigma_t = \kappa_2 \Sigma_{t-1|t-1} + (1-\kappa_2)\, e_t' e_t, \tag{21}$$

$$\Xi_t = (1-\kappa_1^{-1})\, \Sigma^A_{t-1|t-1}, \tag{22}$$

$$\Sigma^A_{t|t-1} = \Sigma^A_{t-1|t-1} + \Xi_t, \tag{23}$$

$$\Sigma_{t|t-1} = z_{t-1}\, \Sigma^A_{t|t-1}\, z_{t-1}' + \Sigma_t. \tag{24}$$

In the updating step, given the information at time t, the parameters are revised as

$$K_t = \Sigma^A_{t|t-1} z'_{t-1} \Sigma^{-1}_{t|t-1}, \tag{25}$$

$$A_{t|t} = A_{t|t-1} + K_t \left(y_t - A_{t|t-1} z_{t-1} \right), \tag{26}$$

$$\Sigma^A_{t|t} = (I - K_t) \Sigma^A_{t|t-1}, \tag{27}$$

$$\Sigma_{t|t} = \kappa_2 \Sigma_{t-1|t-1} + (1 - \kappa_2) e'_{t|t} e_{t|t}, \tag{28}$$

where K_t is the Kalman gain, which governs how much the coefficient estimates A_t are adjusted in each period. When parameter uncertainty $\Sigma^A_{t|t-1}$ is small, the filter places more weight on the prior; when the error variance Σ_t is large, the updated coefficients move closer to the current observation.

The time-varying estimates of A_t and Σ_t feed directly into the generalized connectedness measures of Diebold and Yılmaz (2014). Following Koop, M. H. Pesaran, and Potter (1996) and H. Pesaran and Shin (1998), the TVP-VAR is cast in its VMA representation via the Wold theorem:

$$y_t = \sum_{j=0}^{\infty} B_{jt} e_{t-j}, \qquad B_{jt} = J' M_t^j J, \tag{29}$$

with M_t the $mp \times mp$ companion matrix and J the $mp \times m$ selection matrix. For more details, see Antonakakis, Chatziantoniou, and Gabauer (2020).

The GIRF for a unit shock to variable j at horizon H is:

$$\Psi_{j,t}(H) = \Sigma^{-1/2}_{jj,t} B_{H,t} \Sigma_t e_j, \tag{30}$$

and the normalized GFEVD is:

$$\tilde{\phi}_{ij,t}(H) = \frac{\sum_{h=0}^{H-1} \Psi^2_{ij,t}}{\sum_{j=1}^{m} \sum_{h=0}^{H-1} \Psi^2_{ij,t}}, \tag{31}$$

with $\sum_{j=1}^{m} \tilde{\phi}_{ij,t}(H) = 1$ by construction. Four summary measures follow. The total connectedness index (TCI) is:

$$C_t(H) = \frac{\sum_{i \neq j} \tilde{\phi}_{ij,t}(H)}{m} \times 100. \tag{32}$$

Total directional connectedness transmitted to and received from the rest of the system are:

$$C_{i \to j,t}(H) = \frac{\sum_{j \neq i} \tilde{\phi}_{ji,t}(H)}{\sum_{j=1}^{m} \tilde{\phi}_{ji,t}(H)} \times 100, \tag{33}$$

$$C_{i \leftarrow j,t}(H) = \frac{\sum_{j \neq i} \tilde{\phi}_{ij,t}(H)}{\sum_{i=1}^{m} \tilde{\phi}_{ij,t}(H)} \times 100. \tag{34}$$

Net total directional connectedness, $C_{i,t} = C_{i \to j,t} - C_{i \leftarrow j,t}$, identifies net transmitters ($C_{i,t} > 0$) and net receivers ($C_{i,t} < 0$) of shocks. Net pairwise directional connectedness is

$$\text{NPDC}_{ij,t}(H) = \left(\tilde{\phi}_{ji,t}(H) - \tilde{\phi}_{ij,t}(H)\right) \times 100, \tag{35}$$

where $\text{NPDC}_{ij,t} > 0$ indicates that i is the dominant transmitter in the bilateral relationship with j.

3.4 Data

3.4.1 COVOL estimation

This section describes the data used to estimate the COVOL series for both emerging and developed markets. Multiple institutional

frameworks employ distinct criteria for classifying emerging markets, incorporating economic, financial, and market accessibility dimensions. We adopt the MSCI Emerging Markets Index classification, which in its 2023 composition encompasses 24 countries based on economic development levels and capital market characteristics including liquidity, investability, and accessibility.

Following Engle and Campos-Martins (2023), we employ NYSE-traded ETFs to avoid asynchronicity issues inherent in direct cross-country return analysis. Our selection focuses on ETFs that replicate the main investment opportunities available in each country, utilizing iShares (BlackRock) and Global X (Mirae Asset) funds. Table 1 presents the complete mapping between countries and their corresponding ETF representatives. The Czech Republic, Egypt, and Hungary are excluded due to lack of data.

Table 1
List of Emerging Markets and their Respective ETFs

Country	ETF Ticker	ETF Name
Brazil	EWZ	iShares MSCI Brazil ETF
Chile	ECH	iShares MSCI Chile ETF
China	MCHI	iShares MSCI China ETF
Colombia	GXG	Global X MSCI Colombia ETF
Greece	GREK	Global X MSCI Greece ETF
India	INDA	iShares MSCI India ETF
Indonesia	EIDO	iShares MSCI Indonesia ETF
Korea (South)	EWY	iShares MSCI South Korea ETF
Kuwait	KWT	iShares MSCI Kuwait ETF
Malaysia	EWM	iShares MSCI Malaysia ETF
Mexico	EWW	iShares MSCI Mexico ETF
Peru	EPU	iShares MSCI Peru ETF
Philippines	EPHE	iShares MSCI Philippines ETF
Poland	EPOL	iShares MSCI Poland ETF
Qatar	QAT	iShares MSCI Qatar ETF
Saudi Arabia	KSA	iShares MSCI Saudi Arabia ETF
South Africa	EZA	iShares MSCI South Africa ETF
Taiwan	EWT	iShares MSCI Taiwan ETF
Thailand	THD	iShares MSCI Thailand ETF
Turkey	TUR	iShares MSCI Turkey ETF
United Arab Emirates	UAE	iShares MSCI UAE ETF

To estimate the COVOL of developed markets, we select countries according to the composition of the MSCI Developed Markets Index. The ETF selection follows an analogous procedure to that applied to emerging markets: NYSE-traded funds replicating the main investment opportunities available in each country, primarily from the iShares (BlackRock) family, chosen to mitigate asynchronicity issues inherent in direct cross-country return comparisons. Our final sample comprises 20 developed market countries, presented in Table 2.

Table 2
List of Developed Markets and their Respective ETFs

Country	ETF Ticker	ETF Name
Australia	EWA	iShares MSCI Australia ETF
Austria	EWO	iShares MSCI Austria ETF
Belgium	EWK	iShares MSCI Belgium ETF
Canada	EWC	iShares MSCI Canada ETF
Denmark	EDEN	iShares MSCI Denmark ETF
France	EWQ	iShares MSCI France ETF
Germany	EWG	iShares MSCI Germany ETF
Hong Kong	EWH	iShares MSCI Hong Kong ETF
Ireland	EIRL	iShares MSCI Ireland ETF
Israel	EIS	iShares MSCI Israel ETF
Italy	EWI	iShares MSCI Italy ETF
Japan	EWJ	iShares MSCI Japan ETF
Netherlands	EWN	iShares MSCI Netherlands ETF
Norway	ENOR	iShares MSCI Norway ETF
Singapore	EWS	iShares MSCI Singapore ETF
Spain	EWP	iShares MSCI Spain ETF
Sweden	EWD	iShares MSCI Sweden ETF
Switzerland	EWL	iShares MSCI Switzerland ETF
United Kingdom	EWU	iShares MSCI United Kingdom ETF
United States	SPY	SPDR S&P 500 ETF Trust

Building on this selection, we construct our return series using daily data from Yahoo Finance. Daily gross returns are computed using closing price and dividend information. The sample spans from April 14, 2003, to April 29, 2025, totaling 5,547 trading days. The dataset is unbalanced at the beginning of the sample period, but the entire sample is retained for estimation, as the Expectation-Maximization (EM) algorithm implemented accommodates missing observations by

leveraging all available cross-sectional information.

3.4.2 TVP-VAR estimation

The TVP-VAR analysis is conducted at monthly frequency, as the forgetting factor $\lambda = 0.99$ proposed by Koop and Korobilis (2013) was calibrated for monthly or quarterly data. The COVOL series estimated for each market group are therefore converted to monthly frequency by averaging daily values within each calendar month. We also include monthly logarithmic returns on Brent crude oil and first differences of the VIX, both extracted from Yahoo Finance over the same sample period as the daily data.

4. Results

This section presents the empirical results in two stages. First, we document the properties of the common volatility factor estimated for emerging markets, examining the events associated with its extreme values, and the estimated factor loadings for each country, following Engle and Campos-Martins (2023). Second, we analyze the dynamic relationship between emerging and developed market common volatility within the TVP-VAR connectedness framework of Diebold and Yilmaz (2012), as implemented by Koop and Korobilis (2013) and Antonakakis, Chatziantoniou, and Gabauer (2020).

4.1 Common Volatility in Emerging Markets

To formally assess the presence of common volatility, we proceed to apply the COVOL test to the standardized residuals. The results confirm the presence of significant common volatility across these economies, with $\hat{\rho}_{\hat{\mathbf{e}}^2} = 0.0639$ and a test statistic of $\xi = 14.231$. Our goodness-of-fit analysis yields a negative averaged correlation of $\hat{\rho}_{\hat{\varepsilon}^2} = -0.0163$, suggesting that the common volatility component has been effectively removed. This finding is further supported by the test statistic, which confirms the adequacy of the specification for emerging markets. Figure 2 presents the estimated COVOL series.

Figure 2
Estimated COVOL for Emerging Markets

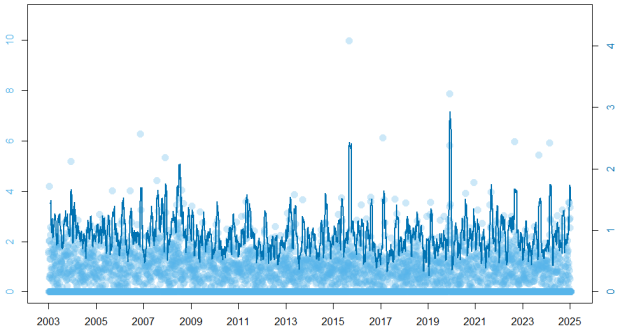

Notes: Light blue dots correspond to individual daily observations (left axis); the solid dark blue line is a 60-day rolling mean (right axis).

Table 3 presents the twenty most extreme common volatility episodes identified in the figure above, revealing a distinctly different pattern of shock transmission compared to the sample used by Engle and Campos-Martins (2023). Most notably, commodity-related events dominate the extreme volatility rankings for emerging markets, with oil price movements featuring prominently across multiple episodes. The most severe volatility spike occurs on December 21, 2015, when oil prices hit an 11-year low, generating an common volatility estimate of 99.76 — nearly double the magnitude of the most extreme event in the full sample (March 2020: 52.75). This amplified sensitivity to commodity shocks reflects emerging markets' structural dependence on natural resource exports and their vulnerability to terms-of-trade fluctuations.

Table 3
Extreme Values - COVOL (Emerging Markets)

Date	Event	$\hat{x}_t$	$\bar{r}_t^{countries}$	r_t^{EEM}	r_t^{brent}
2015-12-21	Oil prices hit 11-year low	99.760	1.567	0.769	-3.939
2020-03-09	COVID-19 lock down & Oil price war	62.193	9.914	7.072	-25.518
2007-02-27	Chinese and European market crashes	39.580	8.157	8.481	-0.099
2017-05-18	Mueller appointed to oversee Russia investigation	37.625	1.293	1.674	-0.097
2022-12-13	Ukraine's allies pledged aid	35.850	1.609	0.800	2.707
2024-06-03	Iran-Israel conflict and OPEC decision (reduction)	34.707	-0.181	-1.047	-3.799
2020-03-12	COVID: President Trump restricts all travel from EU to US	33.892	12.792	10.548	-10.488
2023-12-20	US imposes sanctions on Russian oil price cap	29.988	2.845	3.690	1.591
2008-03-10	Gas and oil prices reach record highs & Iranian suicide attacks	28.524	3.334	1.771	0.638
2004-03-22	Technology stocks fell amid terrorism & OPEC decision (reduction)	26.909	3.257	1.614	-2.239
2007-11-08	Oil hits new record high & Fears rise over U.S. recession	19.685	-0.165	-0.510	-0.476
2021-03-22	COVID: Vaccines show efficacy & EU sanctions China	19.064	1.263	0.296	-0.172
2003-04-24	Iraq war & OPEC decided to reduce oil production	17.709	2.643	1.993	-2.057
2008-11-21	2008 Financial Crisis	16.376	-9.384	-13.456	-1.941
2005-12-23	Chad-Sudan war starts	16.235	1.266	0.515	-1.796
2006-09-20	Fed holds rate steady again & Oil falls on surplus fuel supplies	16.134	-1.331	-2.033	-5.642
2021-12-13	Omicron and inflation shaped expectations for Fed decision	15.762	2.964	3.020	-1.154
2020-11-10	Vaccine hopes	15.362	-0.727	1.146	3.174
2013-08-27	The U.S. considers military action during the Syrian civil war	15.005	3.623	2.329	2.621
2016-11-09	Donald Trump elected	14.192	2.561	3.310	0.939

A recurring pattern in the sample is that most oil-related volatility spikes coincide with sharp oil price declines. Despite the associated uncertainty, average equity returns across emerging markets were often positive on these dates, suggesting that investors may have anticipated policy responses, interpreted falling oil prices as disinflationary, or priced in the terms-of-trade gains accruing to oil-importing economies within the group.

The COVID-19 pandemic, while still significant, exhibits a markedly different impact pattern in the emerging market sample. Only three pandemic-related events appear among the top twenty episodes, compared to their more prominent representation in the full sample analysis. The March 9, 2020 episode (combining COVID-19 lockdowns with the oil price war) ranks second with $\hat{x}_t = 62.19$, while other COVID-related events such as travel restrictions (March 12, 2020: 33.89) and vaccine developments (November 10, 2020: 15.36) appear further down the rankings. This pattern is consistent with emerging markets being more exposed to commodity cycles and geopolitical risk than to the global health shocks that dominated volatility in developed economies.

Figure 3 presents the factor loadings for our emerging market sample under the AGI specification. The results reveal considerable heterogeneity in the degree of integration with the common volatility factor across emerging economies. Gulf Cooperation Council (GCC) countries exhibit the highest factor loadings, with Kuwait (0.290), Qatar (0.278), and UAE (0.228) showing the strongest sensitivities to common volatility shocks.This pattern likely reflects the commodity-driven nature of these economies and their exposure to global energy price dynamics, which constitute a significant component of international financial volatility.

Figure 3
Factor Loadings – Emerging Markets

	$\hat{s}_i$
Kuwait	0.2904
Qatar	0.2777
SDF	0.2714
Taiwan	0.2696
Saudi Arabia	0.2477
Turkey	0.2399
UAE	0.2281
Thailand	0.2173
Indonesia	0.2053
Korea	0.2008
Chile	0.1997
Greece	0.1975
South Africa	0.1957
India	0.1879
China	0.1876
Mexico	0.1836
Peru	0.1818
Colombia	0.1817
Brazil	0.1757
Malaysia	0.1692
Poland	0.1571
Philippines	0.1410

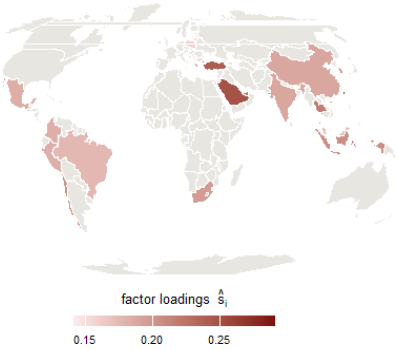

Notes: The table reports the estimated COVOL factor loading $\hat{s}_i$ for each country equity ETF. Countries are ranked in descending order of their loading within each group. SDF denotes the Stochastic Discount Factor portfolio. Higher values indicate greater exposure to the global common volatility factor.

Factor loadings among Asian emerging markets show considerable dispersion. Taiwan ranks among the most exposed economies in the sample (0.270), while Thailand (0.217), Indonesia (0.205), and South Korea (0.201) display moderate sensitivity. The Philippines (0.141) and Malaysia (0.169) exhibit the lowest loadings within the region, consistent with their more domestically oriented financial structures. Latin American markets cluster in the lower-middle range of the distribution: Chile records the highest regional loading (0.200), followed by Peru (0.182), Colombia (0.182), and Brazil (0.176).

Despite their commodity-export orientation, Latin American markets appear less sensitive to the common volatility factor than their Asian and Middle Eastern counterparts. One plausible explanation is that the region's exports are concentrated in distinct commodity classes

— copper (Chile, Peru), oil (Colombia, Brazil), and soybeans (Brazil) — so that country-level returns respond primarily to sector-specific shocks rather than to the common volatility component shared across emerging economies. The elevated weight of domestic political and fiscal risk, well documented in the literature, may further reinforce this pattern.

4.2 Connectedness with Developed Markets

Figure 4 plots, for each group of markets, the cross-sectional average conditional volatility, defined as $\sqrt{(1/N)\sum_{i=1}^{N}\hat{h}_{it}}$, where $\hat{h}_{it}$ is the estimated conditional variance of asset i at time t (Engle and Campos-Martins 2023). Two patterns stand out. First, emerging markets persistently exhibit higher volatility levels than developed markets, with pronounced spikes associated with the 2008–2009 global financial crisis, the 2015–2016 turbulence episode, and the COVID-19 pandemic in 2020. Second, comovement between the two series is visible during the most acute stress episodes, suggesting that global volatility shocks transmit to emerging markets, but with different amplitude.

Figure 4
Comparison of Conditional Volatilities (Emerging vs. Developed)

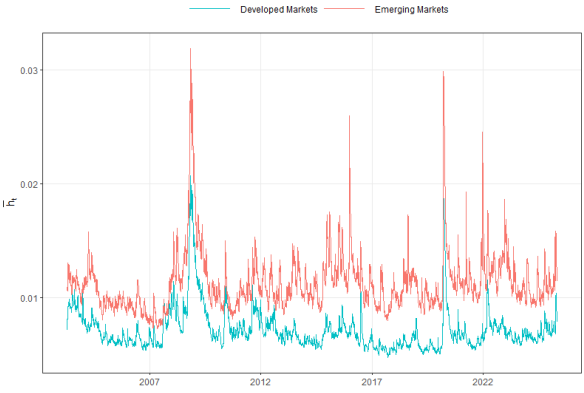

Figure 5 plots the fraction of total variance explained by the first

principal component, obtained from a rolling principal component analysis with a 252-trading-day window applied to the COVOL factors estimated for emerging and developed markets. This metric measures, at each point in time, the degree to which a single latent factor summarizes the joint variation of the two COVOLs — that is, the extent to which common volatility across the two groups of markets collapses into a single dimension. High values indicate that the two factors move in a highly coordinated fashion, while persistent declines in explained variance signal structural divergence between the volatility regimes of the two groups. The series fluctuates predominantly between 65% and 85% over the sample period, suggesting a substantial but not complete degree of systematic comovement.[1]

Figure 5
Systematic Volatility Linkages between Emerging and Developed Markets

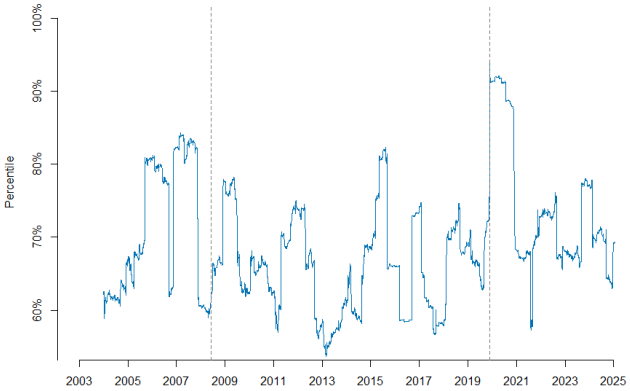

Notes: Dashed vertical lines mark the beginning of the 2008 financial crisis and the COVID-19 pandemic, as dated by FRED recession indicators.

Two episodes concentrate the most pronounced peaks: the 2008–2009 global financial crisis and the COVID-19 pandemic in 2020, during which the variance explained by the first principal component exceeds 90%, indicating that global shocks of exceptional magnitude

[1]The interpretation of COVOL index percentiles as stress regime indicators follows the methodology of V-Lab (NYU Stern Volatility and Risk Institute), available at https://vlab.stern.nyu.edu.

compress cross-group heterogeneity and impose an essentially one-dimensional volatility dynamic. Between these episodes, explained variance retreats and exhibits higher-amplitude fluctuations, suggesting that under moderate stress or in the absence of global shocks, the two COVOLs retain relevant idiosyncratic components and are not adequately described by a single common factor.

Table 4
Connectedness Table – Full-Sample Averages

	Oil Returns	VIX	COVOL (Dev.)	COVOL (Em.)	FROM others
Oil Returns	57.2	13.1	17.0	12.7	42.8
VIX	13.0	56.8	19.8	10.4	43.2
COVOL (Dev.)	12.1	16.3	51.9	19.6	48.1
COVOL (Em.)	12.2	10.4	20.7	56.7	43.3
TO others	37.4	39.9	57.4	42.7	44.3
NET	-5.4	-3.3	9.3	-0.6	

Notes: Each entry θ_{ij} reports the share of the H-step-ahead forecast error variance of variable i attributable to shocks in variable j, averaged over the full sample. TO: total directional connectedness transmitted to others. FROM: total directional connectedness received from others. NET: TO−FROM. TCI: total connectedness index.

The time-varying connectedness dynamics of emerging market COVOL are presented in Figure 6. Panel (a) shows that the TCI exhibits substantial variation over the sample period, with a declining trend between 2008 and mid-2015, followed by a partial recovery and a renewed decline after 2020. This trajectory suggests that the degree of integration of emerging market COVOL with the rest of the system is not stable, which justifies the use of the TVP-VAR over fixed-parameter approaches. Panel (b) details the directional flows: received connectedness (FROM) consistently exceeds transmitted connectedness (TO) for most of the sample, reinforcing the net receiver character of emerging market COVOL identified in the sample average. The most salient episode occurs around 2015–2016, when transmitted connectedness registers a sharp, short-lived spike, possibly associated with the Chinese economic slowdown and the oil market turbulence of that period.

Figure 6
Dynamic Connectedness of COVOL – Emerging Markets

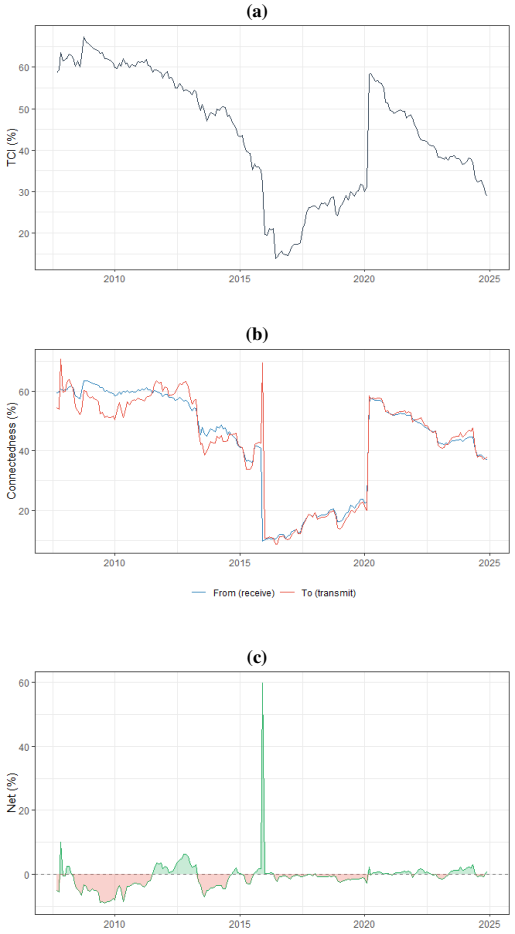

Notes: Panel (a) reports the Total Connectedness Index (TCI) from the TVP-VAR model. Panel (b) shows the directional connectedness received from (FROM) and transmitted to (TO) the remaining variables in the system. Panel (c) shows net directional connectedness (TO minus FROM); positive values indicate net transmission of shocks, negative values indicate net reception.

Panel (c) shows that the net connectedness of emerging market

COVOL remains close to zero in recent years, with episodic positive deviations that dissipate quickly. This pattern is consistent with the argument of Bekaert and Harvey (2023) that emerging markets are progressively more integrated into the global financial system, while retaining risk profiles that structurally distinguish them from developed markets.

5. Final Remarks

This paper investigated the dynamics of common volatility in emerging markets by estimating separate COVOL factors for emerging and developed markets and examining the extent to which emerging market COVOL is driven by factors external to the group. To this end, the stochastic discount factor of Araujo, Galvão, and Issler (2024) was used as the common factor in the conditional mean equation for returns, a choice that anchors identification in no-arbitrage foundations without imposing assumptions about preferences or risk aversion. The dynamic connectedness between the two COVOLs, the VIX, and oil returns was analyzed using a TVP-VAR model with connectedness indices computed via generalized forecast error variance decomposition, following Diebold and Yılmaz (2014) as implemented by Koop and Korobilis (2013).

The results from the first empirical stage show that the most intense episodes of the emerging market factor coincide with stress events in the oil market, suggesting that shocks to this market constitute a relevant amplification channel for common volatility among emerging market assets — a finding consistent with the greater structural dependence of these economies on energy commodities. Rolling principal component analysis indicates that during periods of acute global stress, a single factor accounts for more than 90% of the joint variation in the two COVOLs, whereas under normal conditions explained variance retreats substantially — evidence that cross-group heterogeneity persists outside systemic shock episodes.

The second stage, based on the TVP-VAR, provides evidence on the risk transmission structure of the system. Emerging market COVOL acts predominantly as a net receiver of shocks: on average over the

sample, 43.3% of its variance is accounted for by variables external to the group, with the developed market COVOL contributing the largest share (19.6%), followed by oil returns (12.7%) and the VIX (10.4%). Total system connectedness is not constant: it rises sharply during the 2008 financial crisis and the COVID-19 pandemic, and recedes during periods of greater stability. This pattern implies that emerging market exposure to global risk expands precisely at the moments when international diversification would be most valuable to investors — a result with direct implications for portfolio management with exposure to these markets.

The findings are consistent with the view of Bekaert and Harvey (2023) that emerging markets, despite deepening financial integration, retain risk profiles that structurally distinguish them from developed markets. At the same time, the dependence of emerging market COVOL on developed market common volatility suggests that treating these markets as an independent block for risk allocation purposes understates their exposure to external shocks.

A. Supplementary Tables

Table A1
Factor Loadings (All Countries)

	$\hat{s}_i$ (ECM)	$\hat{s}_i$ (AGI)		$\hat{s}_i$ (ECM)	$\hat{s}_i$ (AGI)
PC1	0.2614		Sweden	0.1269	0.1400
ACWI	0.2498		Taiwan	0.1265	0.1336
SDF		0.2234	UK	0.1265	0.1352
France	0.2172	0.2323	Portugal	0.1229	0.1342
Spain	0.1997	0.2080	Switzerland	0.1182	0.1309
Italy	0.1929	0.2000	Mexico	0.1178	0.1258
Germany	0.1899	0.2096	South Africa	0.1174	0.1219
Netherlands	0.1830	0.2038	Colombia	0.1141	0.1231
Malaysia	0.1788	0.1788	UAE	0.1140	0.1299
Thailand	0.1763	0.1744	Nigeria	0.1131	0.1266
Belgium	0.1757	0.1892	Qatar	0.1127	0.1136
Finland	0.1665	0.1798	Brazil	0.1122	0.1306
USA	0.1634	0.1291	Australia	0.1120	0.1111
Austria	0.1498	0.1568	Israel	0.1104	0.1109
Egypt	0.1484	0.1641	Ireland	0.1088	0.1136
Greece	0.1482	0.1603	Canada	0.1087	0.1168
Indonesia	0.1466	0.1551	Russia	0.1081	0.1114
South Korea	0.1400	0.1510	Denmark	0.1026	0.0985
Singapore	0.1399	0.1420	Pakistan	0.0988	0.1096
Chile	0.1389	0.1409	Peru	0.0955	0.0885
China	0.1363	0.1330	India	0.0937	0.0964
Japan	0.1324	0.1318	Turkey	0.0896	0.0922
Hong Kong	0.1323	0.1386	Vietnam	0.0835	0.0867
Philippines	0.1315	0.1286	Poland	0.0802	0.0793
Norway	0.1304	0.1299	New Zealand	0.0649	0.0643

Table A2
Extreme Values - COVOL (Comparison between all countries)

Date	$\hat{x}_t$ (ECM)	Event	Date	$\hat{x}_t$ (AGI)	Event
March 9, 2020	51.4164	COVID-19 lock down & Oil price war	March 9, 2020	52.7531	COVID-19 lock down & Oil price war
June 24, 2016	49.1903	Brexit referendum	June 24, 2016	47.5135	Brexit Referendum
August 5, 2019	39.4571	China trade war	April 28, 2020	42.7001	COVID Tech sell off
April 28, 2020	38.8836	COVID Tech sell off	September 17, 2001	40.1456	9/11 Market Reopening
September 17, 2001	30.0772	9/11 Market reopening	February 27, 2007	30.2901	Chinese and European stock market crashes
February 27, 2007	26.7564	Chinese and European stock market crashes	November 9, 2016	25.1337	Donald Trump elected
August 24, 2015	23.4313	China Black Monday	August 24, 2015	21.2221	China Black Monday
April 24, 2017	22.0651	Emmanuel Macron elected & Syrian sanctions	April 24, 2017	20.7167	Emmanuel Macron elected & Syrian sanctions
August 5, 2011	18.1861	Speculations about a US credit rate downgrade	March 13, 2020	18.4096	United States enters national emergency over COVID-19
April 9, 2018	18.1160	North Korea considers denuclearization & Missiles strike Syrian air base	August 5, 2011	18.3041	Speculations about a US credit rate downgrade
November 9, 2016	18.0946	Donald Trump elected	April 9, 2018	18.2555	North Korea considers denuclearization & Missiles strike Syrian air base
May 18, 2017	16.8041	Mueller appointed to oversee Russia investigation	May 18, 2017	17.6286	Mueller appointed to oversee Russia investigation
March 13, 2020	16.4795	United States enters national emergency over COVID-19	March 12, 2020	16.3621	COVID: President Trump restricts all travel from EU to US.
March 12, 2020	16.1454	COVID: President Trump restricts all travel from EU to US.	November 9, 2020	15.6854	Pfizer vaccine shows 90% efficacy & Joe Biden elected
November 9, 2020	16.0227	Pfizer vaccine shows 90% efficacy & Joe Biden elected	October 13, 2008	14.3251	Markets react following coordinated crisis recovery packages
October 10, 2008	15.2562	Global Financial Crisis: stock market crash	July 23, 2002	14.0866	Israeli-Palestinian Conflict
March 19, 2020	15.0015	COVID: US Senate proposes $1 trillion stimulus	March 10, 2008	13.9774	Iranian suicide attack kills 5 US soldiers
March 12, 2001	14.7683	Multiple tech firms reported declining revenues	March 18, 2020	13.8833	U.S. Senate approves the Families First Coronavirus Response Act
July 23, 2002	14.5517	Israeli-Palestinian Conflict	May 10, 2004	13.8754	George Bush signs order imposing Syria sanctions
December 17, 2014	14.5281	Peshawar school attack & US reestablishes diplomatic relations with Cuba	January 3, 2001	13.8264	Surprise interest rate cut by the Fed